Published in final edited form as:

Nature. 2011 February 10; 470(7333): 259–263. doi:10.1038/nature09675.

Transmembrane semaphorin signaling controls laminar stratification in the mammalian retina

Ryota L. Matsuoka[1,3], **Kim T. Nguyen-Ba-Charvet**[4,5,6], **Aijaz Parray**[4,5,6], **Tudor C. Badea**[2,3,7], **Alain Chédotal**[4,5,6], and **Alex L. Kolodkin**[1,3]

[1]The Solomon H. Snyder Department of Neuroscience, The Johns Hopkins University School of Medicine, Baltimore, Maryland 21205, USA

[2]Department of Molecular Biology and Genetics, The Johns Hopkins University School of Medicine, Baltimore, Maryland 21205, USA

[3]Howard Hughes Medical Institute, The Johns Hopkins University School of Medicine, Baltimore, Maryland 21205, USA

[4]Institut National de la Santé et de la Recherche Médicale (INSERM), UMR S968, Institut de la Vision, F-75012 Paris, France

[5]Université Pierre et Marie Curie (UPMC) Paris VI, UMR S968, Institut de la Vision, F-75012 Paris, France

[6]Centre National de la Recherche Scientifique (CNRS) UMR 7210, Institut de la Vision, F-75012 Paris, France

Abstract

In the vertebrate retina, establishment of precise synaptic connections among distinct retinal neuron cell types is critical for processing visual information and for accurate visual perception. Retinal ganglion cells (RGCs), amacrine cells, and bipolar cells establish stereotypic neurite arborization patterns to form functional neural circuits in the inner plexiform layer (IPL)1–3: a laminar region that is conventionally divided into five major parallel sublaminae1,2. However, the molecular mechanisms governing distinct retinal subtype targeting to specific sublaminae within the IPL remain to be elucidated. Here, we show that the transmembrane semaphorin Sema6A signals through its receptor PlexinA4 (PlexA4) to control lamina-specific neuronal stratification in the mouse retina. Expression analyses demonstrate that Sema6A and PlexA4 proteins are

Correspondence and requests for materials should be addressed to Alex L. Kolodkin (kolodkin@jhmi.edu).

[1]Present address: Retinal Circuit Development & Genetics Unit, Neurobiology-Neurodegeneration and Repair Laboratory, National Eye Institute, Bethesda, Maryland 20892, USA

Supplementary Information is linked to the online version of the paper at www.nature.com/nature.

Author contributions R.L.M, A.C., and A.L.K. conceived and designed the experiments; R.L.M. performed most of the experiments and data analysis; K.T.N.-B.-C., A.P., and A.C. participated in the phenotypic analyses of *Sema6A* mutant mice and provided *PlexA2*$^{-/-}$ and *PlexB2*$^{-/-}$ mutants; T.C.B performed cholera toxin injections and provided useful suggestions and reagents; R.L.M. and A.L.K. wrote the paper.

expressed in a complementary fashion in the developing retina: Sema6A in most ON sublaminae and PlexA4 in OFF sublaminae of the IPL. Mice with null mutations in *PlexA4* or *Sema6A* exhibit severe defects in stereotypic lamina-specific neurite arborization of tyrosine hydroxylase (TH)-expressing dopaminergic amacrine cells, intrinsically photosensitive RGCs (ipRGCs), and calbindin-positive cells in the IPL. *Sema6A* and *PlexA4* genetically interact *in vivo* with respect to the regulation of dopaminergic amacrine cell laminar targeting. Therefore, neuronal targeting to subdivisions of the IPL in the mammalian retina is directed by repulsive transmembrane guidance cues present on neuronal processes.

Synaptic connections among distinct neuronal cell types are organized in specific laminae within many regions of the nervous system. In the vertebrate retina, RGCs, amacrine cells, and bipolar cells have multiple morphologically distinct subtypes (RGCs: ~20; amacrine cells: ~30, bipolar cells: ~12 subtypes), and each subtype elaborates a characteristic sublaminar connection pattern within the IPL[1,3]. Recent studies show that homophilic cell adhesion molecules, including sidekicks and Dscams, direct sublaminar targeting of distinct amacrine and RGC cell types in the developing chicken retina[4,5]. A mutation in mouse *Dscam* disturbs process self avoidance, mosaic spacing, and stratification of several amacrine cell subtypes[6,7], however it is not clear whether Dscam regulates the stratification of these amacrine cell subtypes directly or whether this is a consequence of other abnormalities in the *Dscam* mutant mouse retina, including disorganization of retinal layers and an expanded IPL. Thus, molecular cues that organize specific laminar stratifications in the mammalian retina have yet to be defined.

The semaphorin family of guidance cues includes secreted and membrane-bound proteins that play key roles in various neuronal developmental processes, including axon guidance and branching, neuronal migration, and dendritic arborization[8]. Multiple classes of semaphorins have been shown to be expressed in the developing mammalian retina[9,10], however, whether or how semaphorins function within the retina is not known.

To assess the *in vivo* roles of semaphorins and their receptors in retinal development, we first conducted expression analyses for conventional semaphorin receptors, *neuropilins* (*Npn-1 and Npn-2*) and *plexins* (*PlexA1–A4, B1–B3, C1, D1*), in the developing mouse retina by *in situ* hybridization. We observed that multiple *plexins* and *neuropilins* are expressed in both overlapping and distinct locations in the developing retina (data not shown). To investigate physiological functions of these semaphorin receptors in retinal development, we analyzed mice harboring targeted mutations in genes encoding each plexin and neuropilin by immunohistochemistry using various retinal markers, including: Pax6, Chx10, Thy-1, TH, calbindin, choline acetyltransferase (ChAT), calretinin, PKCα (Supplementary Fig. 1; data not shown)[11–13]. We identified defects in the stereotypic lamina-specific neurite arborization of tyrosine hydroxylase-positive (TH^+) dopaminergic amacrine cells, and also calbindin-positive cells, in the IPL of adult mice homozygous for a targeted mutation in the gene encoding the PlexA4 receptor[11] (Fig. 1b, d). We utilized division of the IPL into five parallel sublaminae (S1–S5; S5 being closest to the ganglion cell layer) for our analyses, as previously described[1,2]. We observed that dopaminergic amacrine cells, which predominantly stratify in the S1 sublamina of the IPL in wild-type

retinas (Fig. 1a, Supplementary Fig. 2a, 2c), extend aberrant processes into S4/S5 in the *PlexA4*$^{-/-}$ mutant retina (Fig. 1b, Supplementary Fig. 2b, 2d). Similarly, calbindin-positive cells, which typically establish their projections in three strata at the borders of S1 and S2, S2 and S3, S3 and S4 in the IPL of wild-type retinas1 (Fig. 1c), showed aberrant targeting of their processes to S4/S5 in the *PlexA4*$^{-/-}$ retina (Fig. 1d). These sublaminar targeting defects observed in dopaminergic amacrine cells and calbindin-positive cells show full penetrance and expressivity in *PlexA4*$^{-/-}$ mutant retinas (n=10 mutant animals). In order to determine precisely where the aberrant processes of dopaminergic amacrine cells and calbindin-positive cells are localized within the *PlexA4*$^{-/-}$ retina, we performed double-immunolabeling to visualize these two neuronal subtypes along with cells labelled with an antibody directed against calretinin, which marks three strata at the borders of S1 and S2, S2 and S3, S3 and S41 (the localization of calretinin^{+} processes is not disrupted in *PlexA4*$^{-/-}$ retinas; Fig. 1e–f). We found that the aberrant processes of both TH^{+} and calbindin^{+} neuronal subtypes were localized predominantly adjacent to the calretinin^{+} S3/S4 stratification band within S4/S5 in *PlexA4*$^{-/-}$ retinas (Fig. 1g, h). We confirmed that these two populations of mistargeted retinal neurons labelled by anti-TH and anti-calbindin are different retinal subtypes (Supplementary Fig. 3), demonstrating that PlexA4 directs distinct retinal subtype targeting in the IPL *in vivo*. We also found that the calbindin^{+} cells exhibiting neurite arborization defects in *PlexA4*$^{-/-}$ retinas are most likely amacrine cells since these calbindin^{+} cells with aberrant processes in the S4/S5 sublamiane are co-immunolabeled by syntaxin, a pan-amacrine cell marker, but not by Brn3a, a marker for a subset of RGCs (data not shown).

In contrast, other subtypes of RGCs and amacrine cells, including AII amacrine cells labelled with Disabled-1 (Dab-1), vGlut3-positive amacrine cells, cholinergic amacrine cells labelled with ChAT, and R-cadherin-positive cells show normal neurite arborization in the IPL of *PlexA4*$^{-/-}$ mutant retinas (Supplementary Fig. 4). This result further demonstrates that PlexA4 regulation of lamina-specific neurite arborization of retinal neuronal subtypes in the IPL is cell-type specific. Dopaminergic amacrine cell processes, which normally are targeted exclusively to the S1 sublamina (the OFF layer), are misguided in *PlexA4*$^{-/-}$ mutants to the S4/S5 sublaminae (a portion of the ON layer), suggesting that PlexA4 contributes to the segregation of ON and OFF layers within the IPL14.

Recent studies show that dopaminergic amacrine cells co-stratify with, and are synaptically coupled to, M1-type melanopsin intrinsically photosensitive retinal ganglion cells (ipRGCs) in S1 of the mouse IPL15,16. Therefore, we asked whether the abnormality in dopaminergic amacrine cell process stratification affects M1-type ipRGC dendritic arborization in the *PlexA4*$^{-/-}$ retina. We used an antibody directed against the C-terminus of rat melanopsin to label M1-type melanopsin ipRGCs17,18, and we observed aberrant dendritic arborization of M1-type ipRGCs in S4/S5, in addition to stratification within S1 of the IPL in *PlexA4*$^{-/-}$ retina (Fig. 2a, 2b). We also observed that ~75% of aberrant dopaminergic amacrine cell processes (TH-immunoreactive puncta) were co-localized with M1-type ipRGC dendrites (C-terminal melanopsin-immunoreactive puncta) within S4/S5 in *PlexA4*$^{-/-}$ mutant retinas (Fig. 2a”, 2b”, 2c, 2d), suggesting that synaptic connectivity between dopaminergic amacrine cells and M1-type ipRGCs may be still preserved even though these two neuronal

populations have mispositioned processes within the IPL of the *PlexA4*$^{-/-}$ mutant retina. Therefore, PlexA4 is required for precise sublaminar targeting of dopaminergic amacrine cell processes and M1-type ipRGC dendrites within the IPL but may not be essential for synaptic target selection between these two neuronal populations. We examined both the cell number and mosaic patterning of dopaminergic amacrine cells and ipRGCs, and we observed no significant difference between wild-type and *PlexA4*$^{-/-}$ retinas (Supplementary Fig. 5). We also observed no evidence of neuronal process self-avoidance deficits in these cell types in *PlexA4*$^{-/-}$ retinas (Supplementary Fig. 5a–b, e–f). We also found that *PlexA4*$^{-/-}$ RGC axons do not exhibit major projection defects in their trajectories to image forming and non-image forming targets within the brain (Supplementary Fig. 6), nor are errors observed in bipolar cell axon targeting within the IPL (Supplementary Fig. 7).

We next analyzed PlexA4 protein expression using a PlexA4-specific antibody19. We observed no immunostaining with this antibody in *PlexA4*$^{-/-}$ retinas, confirming its specificity (Supplementary Fig. 8a, b). Anti-PlexA4 immunostaining at different postnatal ages shows that PlexA4 is strongly expressed on neuronal processes that predominantly stratify in S1 and S2 of the developing IPL (Fig. 3a, b). We also observed that dopaminergic amacrine cell processes in S1 co-stratified with the upper PlexA4^{+} S1 band (Fig. 3d–d”). To further test if dopaminergic amacrine cells express PlexA4, we performed *in situ* hybridization experiments using a *PlexA4* antisense probe followed by anti-TH immunolabeling. We found that *PlexA4* mRNA is localized to the cell bodies of dopaminergic amacrine cells (26 out of 26 dopaminergic amacrine cells analyzed showed co-localization of TH and *PlexA4* mRNA; Fig. 3e–e”). Taken together, these results strongly suggest PlexA4 functions cell-autonomously in dopaminergic amacrine cells to regulate stratification of this cell type within the IPL. We did not observe PlexA4 protein expression in M1-type ipRGC cell bodies and dendrites (Fig. 3f–f’). This suggests that the M1-type ipRGC dendritic stratification deficit within the IPL of *PlexA4*$^{-/-}$ retinas is a secondary consequence of the developmental defects observed in the IPL of *PlexA4*$^{-/-}$ retinas, supporting a primary role for amacrine cells in directing RGC dendritic stratification3,20,21. Given our observation that dopaminergic amacrine cell processes and M1-type ipRGC dendrites are co-localized in the S4/S5 sublaminae of *PlexA4*$^{-/-}$ retinas, dopaminergic amacrine cells may provide specific cues utilized by M1-type ipRGCs to form selective synaptic contacts.

There are two major classes of potential PlexA4 ligands: secreted Class 3 semaphorins that bind to neuropilin obligate co-receptors and form a holoreceptor complex with PlexA48, and transmembrane Class 6 semaphorins that directly bind to PlexA4 in a neuropilin-independent manner8. We first analyzed neurite arborization of dopaminergic amacrine cells, M1-type ipRGCs, and calbindin-positive cells in *Npn-1*$^{Sema-/Sema-}$ (a *Npn-1* allele that generates a variant Npn-1 protein incapable of responding to Class 3 semaphorin signaling) and *Npn-2*$^{-/-}$ mutant retinas12,13. We observed normal neurite stratification patterns in the IPL for all of these three neuronal subtypes in both *Npn-1*$^{Sema-/Sema-}$ and *Npn-2*$^{-/-}$ retinas (Supplementary Fig. 9), indicating that secreted class 3 semaphorins are unlikely to act as ligands for PlexA4 in the retina.

Transmembrane Class 6 semaphorins, including Sema6A, bind directly to PlexA419. Sema6A induces growth cone collapse of several neuronal subtypes through the PlexA4 receptor *in vitro* and also acts as a repulsive ligand for PlexA4 *in vivo*, regulating hippocampal mossy fiber projections and corticospinal tract decussation19,22. To ask whether Sema6A is a PlexA4 ligand, required for normal retinal development, we first analyzed Sema6A protein expression using a Sema6A-specific antibody23 (Supplementary Fig. 8c–c", d–d"). We found that Sema6A protein is strongly expressed in retinal S3b–S5 sublaminae (S3b being the lower ~1/2 of S3), and expressed at much lower levels in the S1–S3a sublaminae (S3a being the upper ~1/2 of S3) (Fig. 3c). We double-immunolabeled retinal sections with Sema6A and PlexA4 antibodies and found that strong Sema6A and PlexinA4 protein immunoreactivity is detected in adjacent regions of the developing IPL throughout early postnatal retinal development (Fig. 3a–a", Supplementary Fig. 10). These results support the hypothesis that Sema6A functions as a repulsive barrier within the developing IPL for neuronal processes expressing PlexA4, including dopaminergic amacrine cells. We observed Sema6A is not expressed in dopaminergic amacrine cells or M1-type ipRGCs (Fig. 3g, h), consistent with Sema6A serving a non-cell autonomous role in constraining the targeting of processes from these neuronal cell types in the IPL. However, immunolabeling experiments reveal that RGC and amacrine cell subtypes, distinct from ipRGCs and dopaminergic amacrine cells, are the major cellular sources of Sema6A protein in the developing IPL (see Supplementary Figs. 11, 12, 13).

Phenotypic analysis of mice homozygous for a targeted gene-trap mutation in *Sema6A* locus9 shows that *Sema6A*$^{-/-}$ mutants phenocopy the neurite stratification defects in dopaminergic amacrine cells, M1-type ipRGCs, and calbindin-positive cells we observe in *PlexA4*$^{-/-}$ mutant retinas (with full penetrance and expressivity, n=8 *Sema6A*$^{-/-}$ mutant animals, Fig. 4a–f). This result strongly suggests that Sema6A is a functional ligand for PlexA4, required for regulating select aspects of retinal neurite stratification *in vivo*. To further assess the ligand-receptor relationship between Sema6A and PlexA4 in retinal development *in vivo*, we investigated genetic interactions between *PlexA4* and *Sema6A* by analyzing mice doubly heterozygous for *Sema6A* and *PlexA4* mutations. We quantified the number of TH-positive immunoreactive puncta localized in S4/S5 of *Sema6A*$^{+/-}$; *PlexA4*$^{+/-}$ mutant mice (Fig. 4k). In wild-type retinas, TH^{+} immunoreactive puncta in S4/S5 were almost undetectable (Fig. 4g). Mice heterozygous for either *PlexA4* or *Sema6A* mutations did not show a significant increase in the number of the TH^{+} puncta in S4/S5 (Fig. 4h, i). However, *Sema6A*$^{+/-}$; *PlexA4*$^{+/-}$ mutant mice exhibited a markedly increased number of the TH-positive puncta in S4/S5 (Fig. 4j). Therefore, *Sema6A* and *PlexA4* functionally interact *in vivo* and likely act in a common signaling pathway. Together with the complementary expression patterns of Sema6A and PlexA4 in specific regions of the developing IPL, these results strongly support a model in which Sema6A acts as a ligand for the PlexA4 receptor to regulate dopaminergic amacrine cell process targeting in the IPL.

We provide here a demonstration of a molecular cue that directs lamina-specific neurite arborization in the developing mouse retina. We show that Sema6A and its receptor PlexA4 exhibit complementary expression patterns throughout postnatal IPL development, that *Sema6A*$^{-/-}$ mutant mice phenocopy defects in lamina-specific neurite stratification of

specific retinal neuron subtypes observed in *PlexA4*$^{-/-}$ mutant mice, and that they functionally interact *in vivo*. *PlexA4*$^{-/-}$ mutant retinas do not exhibit defects in neurite fasciculation of the retinal cell types that show defects in sublaminar targeting in the IPL (Supplementary Fig. 5), further suggesting that sublaminar targeting in the vertical plane of the mouse retina and neurite arborization in the horizontal plane of the mouse retina are governed by separate mechanisms. Our observations of Sema6A and PlexA4 function in retinal development suggest that initial laminar targeting to broad regions within the developing mouse IPL is directed by a transmembrane guidance cue located on neuronal processes that signals through its receptor, present on other neuronal subtypes. This defines a heterophilic interaction distinct from homophilic adhesive interactions mediated by molecules such as sidekicks and Dscams. Neuronal circuitry mediating two parallel ON/OFF visual pathways is spatially segregated in the IPL of the vertebrate retina1,14, and this spatial segregation plays crucial roles in the effective transmission of distinct light responses to the brain1. Determining how the ON and OFF pathways are segregated at the circuit level is fundamental for understanding visual perception, and our results suggest that these distinct neuronal pathways are established in the IPL through the action of a transmembrane guidance cue and its receptor. Our elucidation of molecular events critical for lamina-specific targeting in the IPL of the mammalian retina may have general implications for understanding mechanisms that govern the establishment of neuronal connectivity, in particular how laminar organization is achieved during neural development.

METHODS SUMMARY

The day of birth in this study is designated as postnatal (P) day 0. The *PlexA4* deficient mouse line and *Sema6A* gene-trap mouse line were previously described9,11. Immunohistochemistry and *in situ* hybridization were performed as previously described13, and the retinal regions we imaged did not include areas near the peripheral edges or the optic nerve head of retinas. See Full Methods for additional detailed experimental procedures, including wholemount retina staining, DRP analysis, quantification of anti-TH and anti-C-terminal melanopsin co-localized puncta, genetic interaction analysis, X-gal staining, cholera toxin injection, and statistical analysis.

Methods

Animals

The day of birth in this study is designated as postnatal (P) day 0. The *PlexA4* deficient mouse line and *Sema6A* gene-trap mouse line were previously described9,11. The *PlexA1*$^{-/-}$, *PlexA2*$^{-/-}$, *PlexA3*$^{-/-}$, *PlexB2*$^{-/-}$, *PlexC1*$^{-/-}$, *Npn-1*$^{Sema-/Sema-}$, and *Npn-2*$^{-/-}$ mice were also described elsewhere11–13,19,24–27. The *PlexB1*$^{-/-}$ and *PlexB3*$^{-/-}$ were obtained from Dr. Peter Mombaerts (unpublished). The *PlexD1*$^{-/flox}$;*nestin cre* mice were generated by Dr. Chenghua Gu (unpublished).

Immunohistochemistry

Eyes were fixed in 4% paraformaldehyde for 1 hr at 4°C, equilibrated in 30% sucrose/PBS and embedded in OCT embedding media (Tissue-Tek). Retinal sections (20–40 μm) were

blocked in 5% fetal bovine serum in 1 X PBS and 0.4% Triton-X100 for 1 hr at room temperature and then incubated overnight at 4°C with primary antibodies: rabbit anti-tyrosine hydroxylase (Millipore at 1:1000), sheep anti-tyrosine hydroxylase (Millipore at 1:400), rabbit anti-N-terminal melanopsin (ATS at 1:2000), rabbit anti-C-terminal rat melanopsin (generous gift from Dr. King-Wai Yau at 1:500)17, rabbit anti-calbindin (Swant at 1:2500), rabbit anti-calretinin (Swant at 1:2500), goat anti-calretinin (Swant at 1:2500), rat anti-R-cadherin (Developmental Studies Hybridoma Bank at 1:200), goat anti-ChAT (Millipore at 1:100), rabbit anti-Dab-1 (generous gift from Dr. Brian Howell at 1:500), mouse anti-PKCα (Millipore at 1:200), mouse anti-Goα (Millipore at 1:500), goat anti-mouse Sema6A (R&D at 1:200), Armenian hamster anti-PlexA4 (generous gift from Dr. Fumikazu Suto at 1:400)19, guinea pig anti-vGlut3 (Millipore at 1:2500), chicken anti-β-gal (Abcam at 1:100), mouse anti-Brn3a (Millipore at 1:20), rabbit anti-Pax6 (Covance at 1:1000), and goat anti-Chx10 (Santa Cruz at 1:50). Sections were washed 6 times for 5 min in 1 X PBS and then incubated with secondary antibodies and TO-PRO-3 (Molecular Probe at 1:400) for 1 hr at room temperature. Sections were washed 6 times for 5min in PBS and coverslips were mounted using vectorshield hard set fluorescence mounting medium (Vector laboratories), and confocal fluorescence images were taken using a Zeiss Axioskop2 Mot Plus, LSM 5 pascal confocal microscope. The regions we imaged did not include areas near the peripheral edges or the optic nerve head of retinas.

Whole-mount retina staining

Enucleated eyes were fixed in 4% paraformaldehyde for 1 hr at 4°C. Whole retina cups were dissected out under a microscope and blocked in PBS containing 5% fetal bovine serum and 0.4% Triton-X100 for 2–3 hr at room temperature. Retina cups were then incubated with primary antibodies in PBS containing 5% fetal bovine serum, 0.4% Triton-X100, and 20% dimethyl sulfoxide (DMSO) for 3–4 days at room temperature. Retinas were washed in PBS + 0.4% Triton-X100 for 7–8 hr at room temperature and incubated with secondary antibodies in PBS containing 5% fetal bovine serum, 0.4% Triton-X100, and 20% DMSO for 24–36 hr at room temperature. Retinas were washed in PBS + 0.4% Triton-X100 for 7–8 hr at room temperature and flat mounted for confocal fluorescence images.

In situ hybridization

In situ hybridization was performed on either fresh frozen or PFA-fixed retina sections (20 μm thickness) as described previously13. Digoxigenin (DIG)-labeled cRNA probes for *PlexA4* and *Sema6A* were used as previously described28. Colorimetric *in situ* hybridization was in some cases followed by fluorescence immunohistochemistry and subsequent pseudocoloring bright field images.

Quantification of anti-TH and anti-C-terminal melanopsin co-localized puncta

Confocal images of two selected regions (112 μm by 112 μm field) from each retina (n=3 retinas from three animals for wild-type and *PlexA4*$^{-/-}$ genotypes) were double-immunostained with anti-TH and anti-C-terminal melanopsin, and the number of anti-TH-immunoreactive puncta co-localized with anti-C-terminal melanopsin in the S4/S5 sublaminae of the IPL was quantified.

Density recovery profile (DRP) analysis

DRP analysis was performed as previously described6,29,30. Confocal images of five selected regions (447 μm by 447 μm field) from each whole-mount retina (n=3 retinas from three animals for wild-type and *PlexA4*$^{-/-}$ genotypes) were used to measure the DRP of dopaminergic amacrine cells or ipRGCs. The retinal regions we used for this analysis did not include the areas near the peripheral edges or the optic nerve head.

X-gal staining

Eyes were fixed in 4% paraformaldehyde at 4°C for 30 min, equilibrated in 30% sucrose/PBS, and embedded in OCT embedding media. Retina sections (20 μm) were stained with 5 mM potassium ferricyanide, 5 mM potassium ferrocyanide, 2 mM $MgCl_2$, and 1 mg/mL X-gal for 1–2 hr at room temperature. Tissue sections were rinsed in PBS and bright-field images were taken.

Genetic interaction analysis

Retinal cross sections (40 μm thickness) from adult wild-type, *PlexA4*$^{+/-}$, *Sema6A*$^{+/-}$, and *Sema6A*$^{+/-}$; *PlexA4*$^{+/-}$ mice were immunostained with anti-TH (n=4 retinas from 4 animals for each genotype). The number of anti-TH-immunoreactive puncta localized in the S4/S5 sublaminae of the IPL in five selected regions (149 μm by 149 μm field) from each retina was quantified. The retinal regions we used for this analysis did not include the areas near the peripheral edges or the optic nerve head.

Cholera toxin injection

Mice were anaesthetized with ketamine. Eyes were injected intravitreally with 1 μl of 2 mg/mL cholera toxin B subunit solution conjugated with Alexa Fluor 488 or 594 (Invitrogen). Four to five days after injection, mice were perfused intracardially with 4% paraformaldehyde in PBS and brains were isolated. 100 μm brain sections were cut using a vibratome, and fluorescence images were taken.

Statistical analysis

Statistical differences for mean values among multiple groups were determined using Tukey's multiple comparison test. The criterion for statistical significance was set at $p < 0.05$. Error bars are SEM.

Supplementary Material

Refer to Web version on PubMed Central for supplementary material.

Acknowledgements

We thank Dr. King-Wai Yau for the C-terminal melanopsin antibody, Dr. Fumikazu Suto for the PlexA4 antibody, Dr. Brian Howell for the Dab-1 antibody, Dr. Yutaka Yoshida for the *PlexA1*$^{-/-}$ eyes, Dr. Peter Mombaerts for the *PlexB1*$^{-/-}$ and *PlexB3*$^{-/-}$ mice (unpublished), Dr. Chenghua Gu for the *PlexD1*$^{-/flox}$;*nestin cre* (unpublished) eyes, and Dr. Marc Tessier-Lavigne for the *PlexA4*$^{-/-}$ mice. We also thank Drs. Jeremy Nathans, Samer Hattar, Kenji Mandai, and Martín Riccomagno for helpful comments on the manuscript and discussions, and members of Kolodkin laboratory for assistance. This work was supported by R01 NS35165 to A.L.K.; a predoctoral fellowship from the Nakajima Foundation to R.L.M; the Fondation pour la Recherche Médicale (Programme équipe FRM) to

A.C.; the Fondation Retina France to K.T.N.-B.-C.; and a Ph.D. fellowship from the Paris School of Neuroscience (ENP) to A.P.. A.L.K. is an investigator of the Howard Hughes Medical Institute.

References

1. Wassle H. Parallel processing in the mammalian retina. Nat Rev Neurosci. 2004; 5:747–757. [PubMed: 15378035]
2. Sanes JR, Zipursky SL. Design principles of insect and vertebrate visual systems. Neuron. 2010; 66:15–36. [PubMed: 20399726]
3. Huberman AD, Clandinin TR, Baier H. Molecular and cellular mechanisms of lamina-specific axon targeting. Cold Spring Harb Perspect Biol. 2010; 2:a001743. [PubMed: 20300211]
4. Yamagata M, Weiner JA, Sanes JR. Sidekicks: synaptic adhesion molecules that promote lamina-specific connectivity in the retina. Cell. 2002; 110:649–660. [PubMed: 12230981]
5. Yamagata M, Sanes JR. Dscam and Sidekick proteins direct lamina-specific synaptic connections in vertebrate retina. Nature. 2008; 451:465–469. [PubMed: 18216854]
6. Fuerst PG, Koizumi A, Masland RH, Burgess RW. Neurite arborization and mosaic spacing in the mouse retina require DSCAM. Nature. 2008; 451:470–474. [PubMed: 18216855]
7. Fuerst PG, Harris BS, Johnson KR, Burgess RW. A novel null allele of mouse DSCAM survives to adulthood on an inbred C3H background with reduced phenotypic variability. Genesis. 2010
8. Tran TS, Kolodkin AL, Bharadwaj R. Semaphorin regulation of cellular morphology. Annu Rev Cell Dev Biol. 2007; 23:263–292. [PubMed: 17539753]
9. Leighton PA, et al. Defining brain wiring patterns and mechanisms through gene trapping in mice. Nature. 2001; 410:174–179. [PubMed: 11242070]
10. de Winter F, Cui Q, Symons N, Verhaagen J, Harvey AR. Expression of class-3 semaphorins and their receptors in the neonatal and adult rat retina. Invest Ophthalmol Vis Sci. 2004; 45:4554–4562. [PubMed: 15557467]
11. Yaron A, Huang PH, Cheng HJ, Tessier-Lavigne M. Differential requirement for Plexin-A3 and -A4 in mediating responses of sensory and sympathetic neurons to distinct class 3 Semaphorins. Neuron. 2005; 45:513–523. [PubMed: 15721238]
12. Gu C, et al. Neuropilin-1 conveys semaphorin and VEGF signaling during neural and cardiovascular development. Dev Cell. 2003; 5:45–57. [PubMed: 12852851]
13. Giger RJ, et al. Neuropilin-2 is required in vivo for selective axon guidance responses to secreted semaphorins. Neuron. 2000; 25:29–41. [PubMed: 10707970]
14. Famiglietti EV Jr, Kolb H. Structural basis for ON-and OFF-center responses in retinal ganglion cells. Science. 1976; 194:193–195. [PubMed: 959847]
15. Viney TJ, et al. Local retinal circuits of melanopsin-containing ganglion cells identified by transsynaptic viral tracing. Curr Biol. 2007; 17:981–988. [PubMed: 17524644]
16. Zhang DQ, et al. Intraretinal signaling by ganglion cell photoreceptors to dopaminergic amacrine neurons. Proc Natl Acad Sci U S A. 2008; 105:14181–14186. [PubMed: 18779590]
17. Hattar S, Liao HW, Takao M, Berson DM, Yau KW. Melanopsin-containing retinal ganglion cells: architecture, projections, and intrinsic photosensitivity. Science. 2002; 295:1065–1070. [PubMed: 11834834]
18. Pires SS, et al. Differential expression of two distinct functional isoforms of melanopsin (Opn4) in the mammalian retina. J Neurosci. 2009; 29:12332–12342. [PubMed: 19793992]
19. Suto F, et al. Interactions between plexin-A2, plexin-A4, and semaphorin 6A control lamina-restricted projection of hippocampal mossy fibers. Neuron. 2007; 53:535–547. [PubMed: 17296555]
20. Stacy RC, Wong RO. Developmental relationship between cholinergic amacrine cell processes and ganglion cell dendrites of the mouse retina. J Comp Neurol. 2003; 456:154–166. [PubMed: 12509872]
21. Kay JN, et al. Transient requirement for ganglion cells during assembly of retinal synaptic layers. Development. 2004; 131:1331–1342. [PubMed: 14973290]

22. Runker AE, Little GE, Suto F, Fujisawa H, Mitchell KJ. Semaphorin-6A controls guidance of corticospinal tract axons at multiple choice points. Neural Dev. 2008; 3:34. [PubMed: 19063725]
23. Kerjan G, et al. The transmembrane semaphorin Sema6A controls cerebellar granule cell migration. Nat Neurosci. 2005; 8:1516–1524. [PubMed: 16205717]
24. Yoshida Y, Han B, Mendelsohn M, Jessell TM. PlexinA1 signaling directs the segregation of proprioceptive sensory axons in the developing spinal cord. Neuron. 2006; 52:775–788. [PubMed: 17145500]
25. Cheng HJ, et al. Plexin-A3 mediates semaphorin signaling and regulates the development of hippocampal axonal projections. Neuron. 2001; 32:249–263. [PubMed: 11683995]
26. Friedel RH, et al. Plexin-B2 controls the development of cerebellar granule cells. J Neurosci. 2007; 27:3921–3932. [PubMed: 17409257]
27. Pasterkamp RJ, Peschon JJ, Spriggs MK, Kolodkin AL. Semaphorin 7A promotes axon outgrowth through integrins and MAPKs. Nature. 2003; 424:398–405. [PubMed: 12879062]
28. Suto F, et al. Plexin-a4 mediates axon-repulsive activities of both secreted and transmembrane semaphorins and plays roles in nerve fiber guidance. J Neurosci. 2005; 25:3628–3637. [PubMed: 15814794]
29. Rodieck RW. The density recovery profile: a method for the analysis of points in the plane applicable to retinal studies. Vis Neurosci. 1991; 6:95–111. [PubMed: 2049333]
30. Rockhill RL, Euler T, Masland RH. Spatial order within but not between types of retinal neurons. Proc Natl Acad Sci U S A. 2000; 97:2303–2307. [PubMed: 10688875]

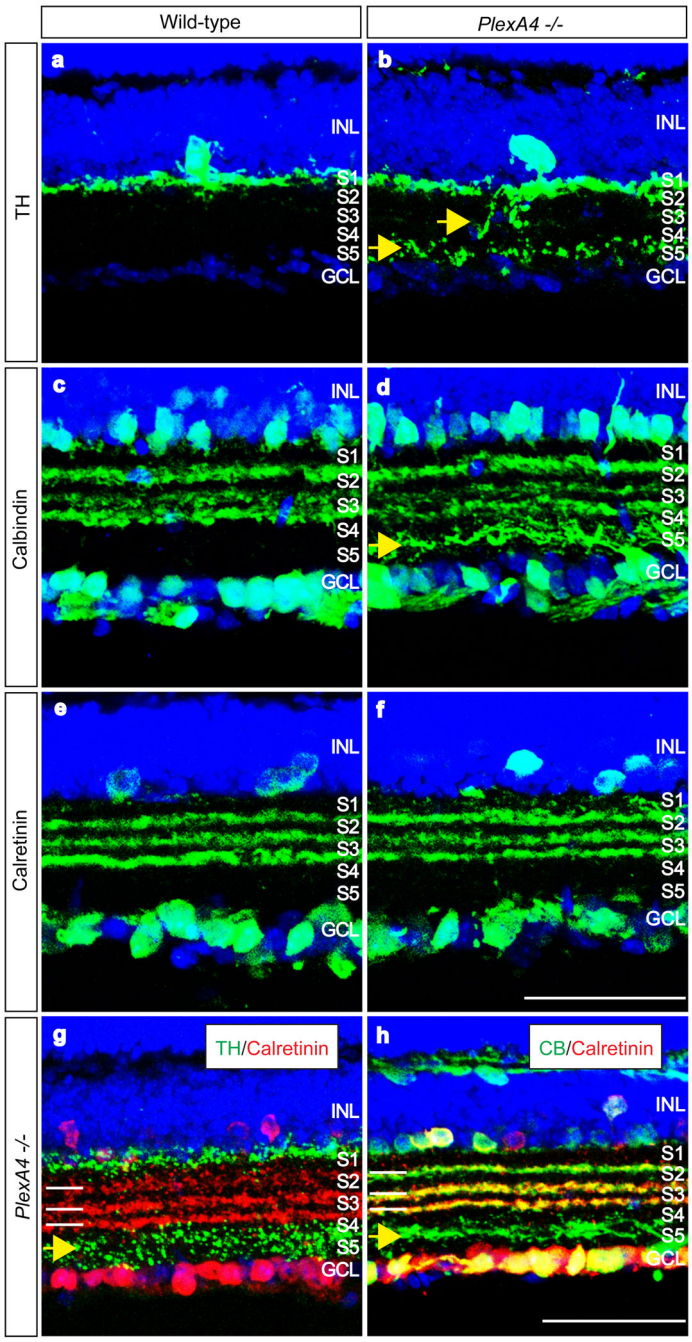

Figure 1. PlexinA4 directs lamina-specific neurite arborization of dopaminergic amacrine cells and calbindin-positive cells in the IPL *in vivo*

a–h, Wild-type (**a, c, e**) and *PlexA4*$^{-/-}$ (**b, d, f**) adult retina sections were immunostained with antibodies against TH (**a, b**), calbindin (**c, d**), and calretinin (**e, f**). In *PlexA4*$^{-/-}$ retinas, TH-positive dopaminergic amacrine cells and calbindin-positive cells exhibit defects in lamina-specific neurite arborization (yellow arrows, **b** and **d**, n=10 *PlexA4*$^{-/-}$ animals). In wild-type retinas, dopaminergic amacrine cell processes are observed predominantly in the S1 sublamina of the IPL (**a**). In contrast, aberrant punctate immunostaining is detected in the

S4/S5 sublaminae, in addition to S1, in all *PlexA4*$^{-/-}$ retinas examined (**b**). The normal stratification of calbindin-positive cells in the IPL (**c**) is disrupted in *PlexA4*$^{-/-}$ retinas, resulting in aberrant processes in S4/S5 (**d**). Calretinin-positive cells show normal sublaminar stratification in the IPL of *PlexA4*$^{-/-}$ retinas (**e–f**).
g and **h**, *PlexA4*$^{-/-}$ adult retina sections double-immunostained with anti-calretinin (white bars) and anti-TH (**g**), or anti-calretinin and anti-calbindin (CB) (**h**). Aberrant processes in *PlexA4*$^{-/-}$ retinas from dopaminergic amacrine cells, and also from calbindin-positive cells, are found adjacent to and closer to the GCL than the calretinin-positive processes that lie between S3 and S4 in the IPL (yellow arrows). Scale bars: 50 μm in **h** for **a, b, g, h**, and in **f** for **c–f**.

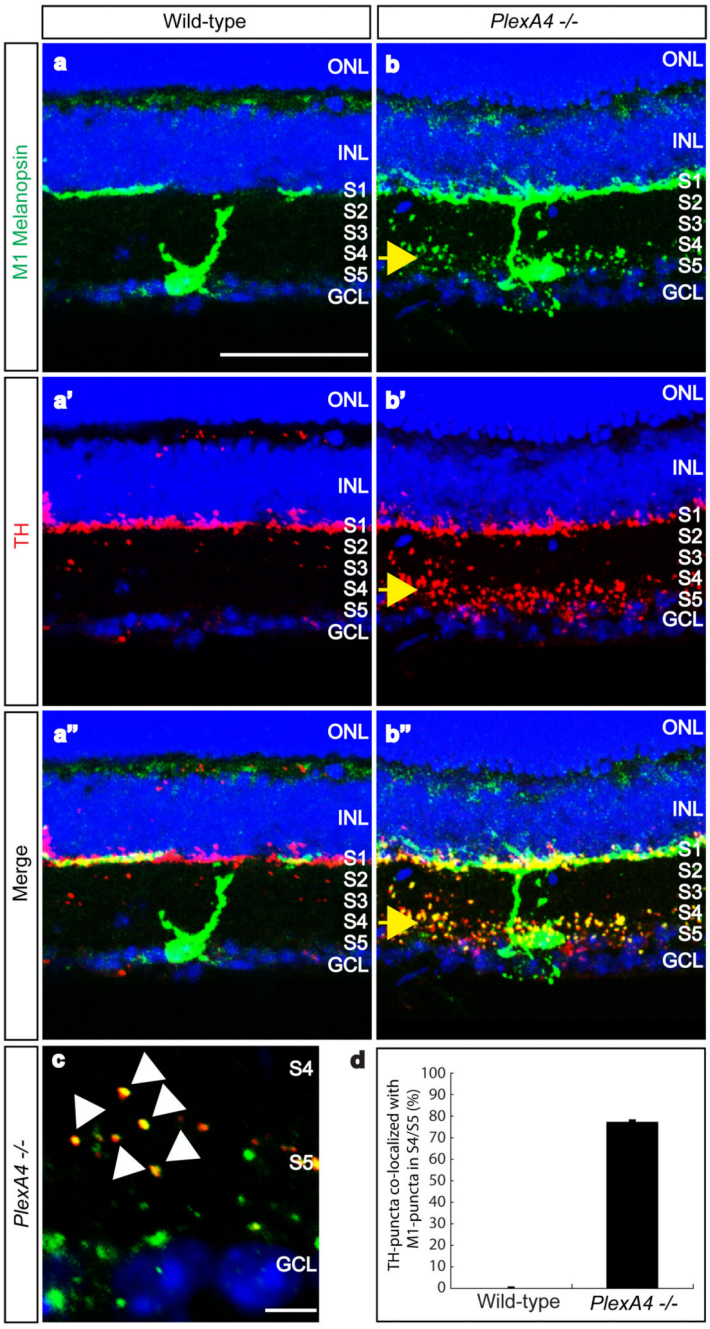

Figure 2. PlexinA4 controls dendritic targeting of M1-type ipRGCs within the IPL, but not co-localization of dopaminergic amacrine cell and ipRGC processes

a–a", b–b", Double-immunostaining using antibodies directed against the C-terminus of rat melanopsin (**a** and **b**, green) and against TH (**a'** and **b'**, red) of wild-type (**a–a"**) and *PlexA4*$^{-/-}$ (**b–b"**) adult retina sections (merged in **a"** and **b"**). Ectopic dendritic processes of M1-type ipRGCs were observed in the S4/S5 sublaminae of *PlexA4*$^{-/-}$ retinas, as were aberrant dopaminergic amacrine processes (yellow arrows, **b–b"**, n=4 mutant animals).

Wild-type M1-type ipRGC dendritic processes and dopaminergic amacrine cell processes are only observed in S1 (**a–a”**).

c, High-magnification of S4/S5 in *PlexA4*$^{-/-}$ retinas double-immunostained with anti-C-terminal melanopsin and anti-TH. Most TH-positive puncta are co-localized with melanopsin-positive puncta (white arrowheads).

d, Quantification of ectopic TH-positive puncta co-localized with the ectopic M1-type melanopsin puncta in S4/S5 of *PlexA4*$^{-/-}$ retinas. Nearly 76% (194 TH-positive puncta among a total of 254 puncta) of the ectopic TH-positive puncta were co-localized with ectopic M1-type melanopsin puncta in S4/S5 (76.4±1.2% co-localization). In wild-type retinas, almost no TH-positive puncta were observed in S4/S5. Error bar indicates SEM (n=3 animals per genotype). Scale bars: 50 μm in **a** for **a–a”** and **b–b”**, and 5 μm in **c**.

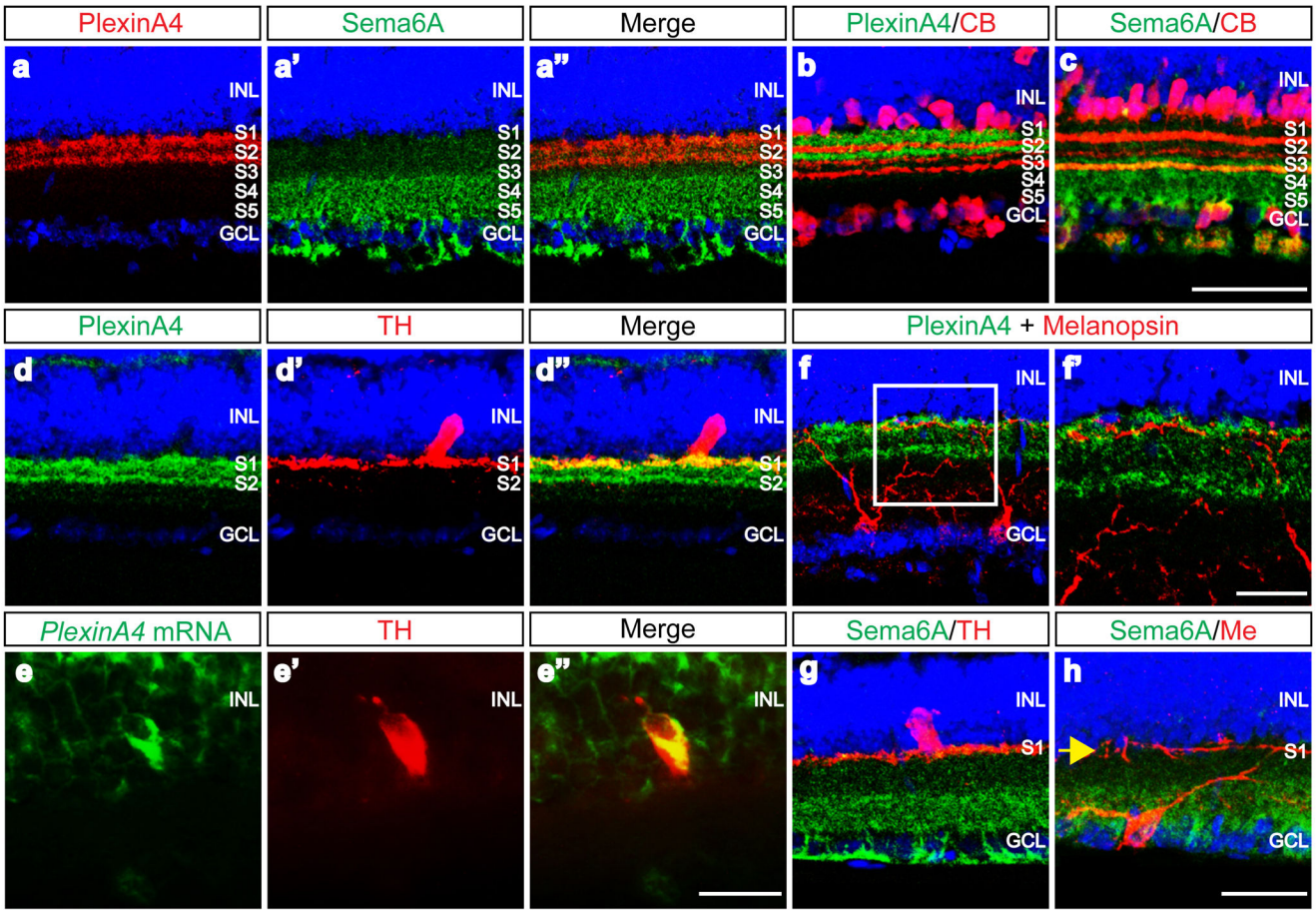

Figure 3. PlexinA4 and Sema6A exhibit complementary protein expression in the developing mouse retina

a–a”, P14 retina section double-immunostained with anti-PlexA4 (**a**, red) and anti-Sema6A (**a’**, green) (merged in **a”**). Strong Sema6A immunoreactivity in the IPL was observed in ~one-half of S3 and throughout S4 and S5, whereas PlexA4 expression is stratified in two distinct layers in S1 and S2.

b, P14 retina section double-immunostained with anti-PlexA4 (green) and anti-calbindin (CB, red) shows PlexA4 protein localization in S1/S2 sublaminae relative to calbindin-positive neuronal processes.

c, P14 retina section double-immunostained with anti-Sema6A (green) and anti-calbindin (CB, red) shows Sema6A protein localization in the S3–S5 relative to calbindin-positive neuronal processes.

d–d”, P14 retina section double-immunostained with anti-PlexA4 (**d**, green) and anti-TH (**d’**, red), revealing co-localization of PlexA4 and TH immunoreactivity in S1 of the IPL (merged in **d”**).

e–e”, P14 retina section hybridized with *PlexA4* antisense probe (**e**, green) followed by anti-TH immunolabeling (**e’**, red, merged in **e”**). *PlexA4* mRNA is localized to the cell body of dopaminergic amacrine cells (of 26 TH-positive amacrine cells scored, all were positive for *PlexA4* mRNA).

f and **f'**, P14 retina section double-immunostained with anti-PlexA4 (green) and anti-N-terminal melanopsin (red), which labels multiple ipRGC subtypes18 (**f**; high magnification of the area in the white square shown in **f')**. PlexA4 immunoreactivity was not observed in the cell bodies or dendrites of ipRGCs.

g and **h**, P14 retina sections double-immunostained with anti-Sema6A (green) and anti-TH (**g**, red) or anti-N-terminal melanopsin (Me) (**h**, red). Sema6A protein was not observed in cell bodies, or processes, of dopaminergic amacrine cells and ipRGCs (M1-type ipRGC dendritic processes in the S1 indicated by yellow arrow in **h**).

Scale bars: 50 μm in **c** for **a–a"**, **b**, **c**, 50 μm in **h** for **d–d"**, **f**, **g–h**, 20 μm in **e"** for **e–e"**, and 20 μm in **f'**.

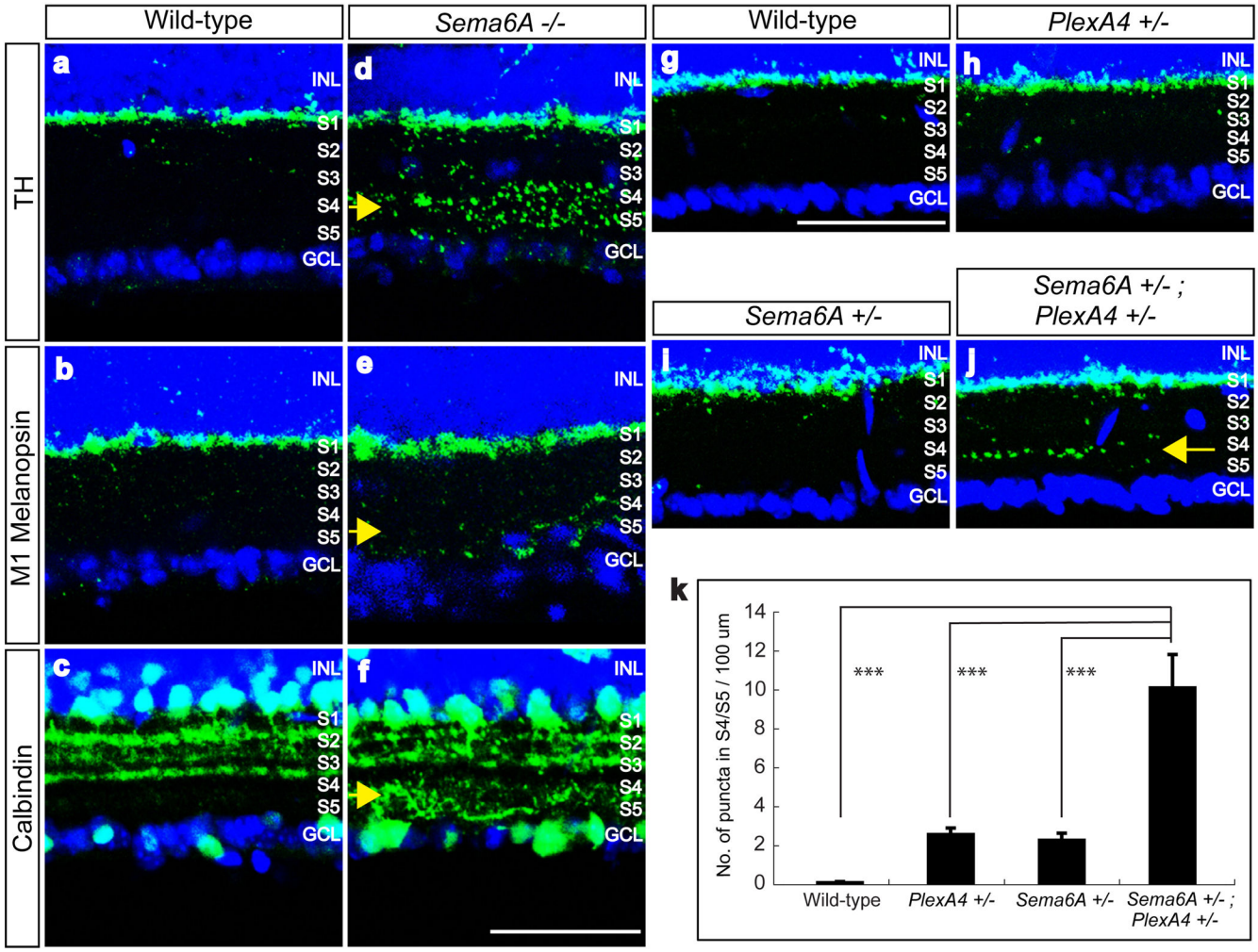

Figure 4. Sema6A signaling through the PlexinA4 receptor directs retinal sublaminar targeting

a–f, Wild-type (**a–c**) and *Sema6A*$^{-/-}$ (**d–f**) adult retina sections were immunostained with antibodies against TH (**a, d**), C-terminal melanopsin (**b, e**), and calbindin (**c, f**). *Sema6A*$^{-/-}$ retinas recapitulate the lamina-specific neurite arborization defects of dopaminergic amacrine cells, M1-type ipRGCs, and calbindin-positive cells (yellow arrows) observed in *PlexA4*$^{-/-}$ retinas (n=8 *Sema6A*$^{-/-}$ animals).

g–j, Wild-type (**g**), *PlexA4*$^{+/-}$ (**h**), *Sema6A*$^{+/-}$ (**i**), and *Sema6A*$^{+/-}$; *PlexA4*$^{+/-}$ (**j**) adult retina sections were immunostained with anti-TH.

k, Quantification of ectopic TH-positive puncta detected in the S4/S5 sublaminae in wild-type (**g**), *PlexA4*$^{+/-}$ (**h**), *Sema6A*$^{+/-}$ (**i**), and *Sema6A*$^{+/-}$; *PlexA4*$^{+/-}$ (**j**) sections (n=4 animals for each genotype). An increased number of TH-positive puncta was observed in S4/S5 in *Sema6A*$^{+/-}$; *PlexA4*$^{+/-}$ retinas (10.1±1.7 puncta per 100 μm, yellow arrow, **j**) as compared to the other three genotypes (0.1±0.1 puncta per 100 μm, wild-type 2.6±0.3 puncta per 100 μm, *PlexA4*$^{+/-}$; 2.3±0.4 puncta per 100 μm, *Sema6A*$^{+/-}$; **g–i**). Error bars are SEM. *** indicates $P < 0.01$ by Tukey's multiple comparison test.

Scale bars: 50 μm in **f** for **a–f**, and in **g** for **g–j**.